Supporting Information

Puccini et al. 10.1073/pnas.1311947110

SI Materials and Methods

Cell Culture. Freshly isolated thymic lymphomas, spleens, and thymuses were homogenized, filtered through a 40-μm nylon mesh, and incubated in red blood cell lysis buffer (155 mM NH_4Cl, 10 mM $NaHCO_3$) for 5 min. Cells were grown at 37 °C with 10% CO_2 in high-glucose Dulbecco modified Eagle medium (Sigma-Aldrich) supplemented with 10% (vol/vol) FBS (JHR Biosciences), 50 μM β-mercaptoethanol (Amersham Biosciences), nonessential amino acid mix (Sigma-Aldrich), 0.2 mM L-glutamine (Sigma-Aldrich), 15 mM Hepes (Sigma-Aldrich), and 100 μM penicillin/streptomycin (Sigma-Aldrich). Freshly isolated splenocyte and thymocyte cell suspensions were stimulated with 5 μg/mL Concanavalin A (Sigma-Aldrich) and 100 U/mL recombinant mouse IL-2 (Cell Signaling) for 48 and 24 h, respectively, before Colcemid (20 ng/mL) treatment for cytogenetic analysis. EL4 thymoma mouse cell line was obtained from Simon Apte, (Queensland Institute of Medical Research, Brisbane, Australia) and was maintained in RPMI medium supplemented with 6% (vol/vol) FCS and 100 μM penicillin/streptomycin (Sigma-Aldrich).

Telomere FISH. Metaphase spreads were prepared from freshly isolated lymphoma cell suspensions as previously described (1). Telomere FISH was performed on metaphase spreads by using the Telomere PNA FISH Kit/Cy3 (DAKO) according to the manufacturer's instructions. Images were captured by using an epifluorescence microscope (model BX51; Olympus) and a camera (U0CMAD3/CVM300; Olympus), then manually merged by using Adobe Photoshop CS5.

Timed Pregnancies and Embryo Dissections. Females were set up in timed pregnancies and monitored twice daily for the presence of a copulation plug, at which time they were designated as embryonic day 0.5. Pregnant females were euthanized at 18.5 d postcoitum. Embryos were extracted and decapitated, and heads and bodies were fixed in Bouin solution (Sigma-Aldrich) for 2 d, followed by daily washes in 70% (vol/vol) ethanol for 7 d. Fixed embryos were processed and embedded in paraffin, sectioned, and stained with H&E by standard procedures. Digital images were acquired by using a NanoZoomer (Hamamatsu).

Flow Cytometry. For DNA content analysis, 1×10^6 lymphoma cells were seeded into six-well plates, cultured for 24 h, and then treated with 10 μM menadione (Sigma-Aldrich) or exposed to 5 Gy γ-radiation from a ^{137}Cs source. At the indicated times, cells were fixed in 70% (vol/vol) ethanol and stored at −20 °C. Cells were then treated with 40 μg/mL RNaseA (Roche), stained with 25 μg/mL propidium iodide (Sigma-Aldrich), and then analyzed on an FC500 flow cytometer (Beckman Coulter). Cells with a sub-G1 DNA content were gated as apoptotic. At least 50,000 events were recorded per sample. For immunophenotyping, freshly isolated thymic lymphoma cells were blocked in 10% (vol/vol) normal mouse serum for 30 min at room temperature. Cells were then incubated with the following conjugated antibodies (diluted 1:100 in 1% BSA/PBS solution) for 1 h on ice in the dark: CD4-Alexa 488, CD8a-PE, and CD90.2-PE (BD Biosciences). After washing in blocking solution, live cells were analyzed on an FC500 flow cytometer (Beckman Coulter). At least 20,000 events were recorded per sample. Data analysis was performed by using FCS Express Flow Cytometry Research Edition, version 4 (DeNovo Software).

Quantitative PCR. First-strand cDNA synthesis was performed with the High Capacity cDNA Reverse Transcription Kit (Applied Biosciences) by using oligo-dT primers and total RNA extracted from frozen thymic lymphoma tissue using TRIzol reagent (Life Technologies). Real-time PCR was performed on a Rotor-Gene 3000 (Corbett Research) by using RT^2 Real-Time SYBR Green/ROX PCR Master Mix (Qiagen) per the manufacturer's instructions. Each gene was analyzed in two or three independent PCR runs. Expression was normalized to β-actin by using the $2^{-\Delta Ct}$ method. The following primer sequences were used for amplification of mouse genes:

Sod2: 5′-ATTAACGCGCAGATCATGCA-3′, 5′-TGTCCCCCACCATTGAACTT-3′;
Prdx3: 5′-GCTCTGGTCCTCGGTTGCTC-3′, 5′-AGGCTGACTTTCCTTGGGCAG-3′;
Cat: 5′-TCTTCGTCCCGAGTCTCTCC-3′, 5′-CCTGGTCGGTCTTGTAATGG-3′;
Sesn1: 5′-CCGTGGTTCTGCTCACACAC-3′, 5′-CACTTACCGAAGCATTTCCTGC-3′;
Sesn2: 5′-TAGCCTGCAGCCTCACCTAT-3′, 5′-TATCTGATGCCAAAGACGCA-3′;
β-*actin*: 5′-GATCATTGCTCCTCCTGAGC-3′, 5′-AGTCCGCCTAGAAGCATTTG-3′.

Hematological Analysis. Blood lymphocyte counts were measured in peripheral blood extracted from tumor-laden mice via cardiac puncture. Automated analysis was performed at the Department of Clinical Pathology, SA Pathology (Adelaide, Australia).

Sample Preparation for Protein Carbonyl and 8-Hydroxy-2-Deoxy Guanosine Measurements. Protein carbonyl levels (expressed as nanomoles per milligram of protein) were measured in total protein lysates prepared from frozen thymic lymphoma tissue or freshly isolated splenocyte and thymocyte cell pellets. Tissues were homogenized in 25 mM Tris·HCl, pH 7.4, 150 mM NaCl, 1% nonyl phenoxylpolyethoxylethanol, 1% sodium deoxycholate, and 0.1% sodium dodecyl sulfate in the presence of protease/phosphatase inhibitor mixture (Thermo Scientific). Protein concentration was determined by using the Protein Assay reagent (BioRad). 8-Hydroxy-2-deoxy guanosine levels (expressed as picograms per microgram of DNA) were measures in genomic DNA extracted from frozen thymic lymphoma tissue. Tissues were digested in 50 mM Tris·HCl, 50 mM EDTA, pH 8.0, 0.125% SDS, 800 μg/μL proteinase K for 3 h at 55 °C. Genomic DNA was purified by phenol chloroform extraction, digested with nuclease P1 (Sigma-Aldrich) for 1 h at 37 °C, and quantified by using a NanoDrop spectrophotometer (Thermo Scientific).

Immunoblotting. Lymphoma cell lines were cultured for 24 h, then exposed to γ-radiation (5 Gy) from a ^{137}Cs source. Cell pellets from lymphoma cell lines or frozen lymphoma tissues were homogenized in lysis buffer containing 50 mM Tris·HCl (pH 7.4), 150 mM NaCl, 2 mM EGTA, 2 mM EDTA, 25 mM sodium fluoride, 25 mM β-glycerophosphate, 0.1 mM sodium orthovanadate, 0.1 mM PMSF, 0.2% Triton X-100, 0.3% Nonidet P-40, and protease inhibitors (Roche Diagnostics) and incubated on ice for 30 min. Whole protein extracts were resolved by SDS/PAGE and transferred to PVDF membranes. Membranes were immunoblotted with the following antibodies: anti-SMC1 rabbit polyclonal antibody (1:1,000 dilution; Novus Biologicals), anti-SMC1 pS957 rabbit monoclonal antibody (clone EP2857Y; 1:1,000 dilution; GeneTex), anti-KAP-1 rabbit polyclonal antibody (1:1,000

dilution; Novus Biologicals), anti-KAP-1 pS824 rabbit polyclonal antibody (1:1,000 dilution; Novus Biologicals), anti-Chk1 mouse monoclonal antibody (clone DCS-310; 1:500 dilution; Thermo Scientific), anti-Chk1 pS317 rabbit polyclonal (1:500 dilution; Thermo-Scientific), anti-p53 mouse monoclonal antibody (clone 1C12; 1:1,000 dilution; Cell Signaling Technology), anti-p21 mouse monoclonal antibody (clone SX118; 1:500 dilution; BD Biosciences), and anti–β-actin mouse monoclonal antibody (clone AC-15; 1:2,000 dilution; Sigma-Aldrich). Alkaline phosphatase, Cy5, and HRP-conjugated secondary antibodies (Millipore/GE Healthcare) were used for detection. Proteins were visualized by using ECF and ECL substrates (GE Healthcare).

1. Dorstyn L, et al. (2012) Caspase-2 deficiency promotes aberrant DNA-damage response and genetic instability. *Cell Death Differ* 19(8):1288–1298.

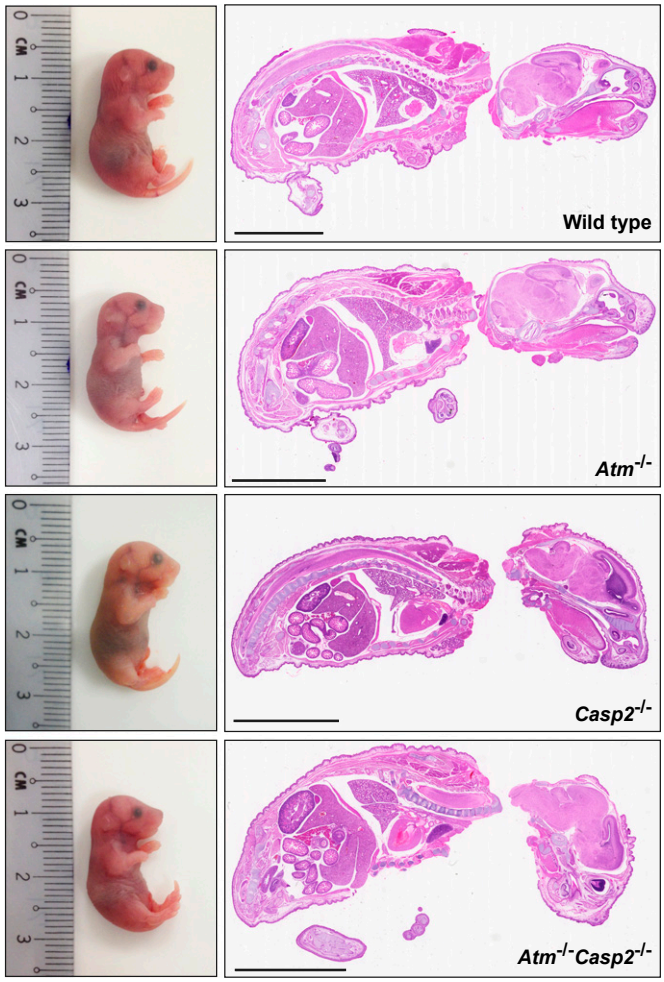

Fig. S1. Gross morphology of *Atm*$^{-/-}$*Casp2*$^{-/-}$ embryos. Representative images of H&E-stained, embryonic day 18.5 sagittal sections of the indicated genotypes. Representative images of live embryos are also shown. (Scale bar: 5 mm.)

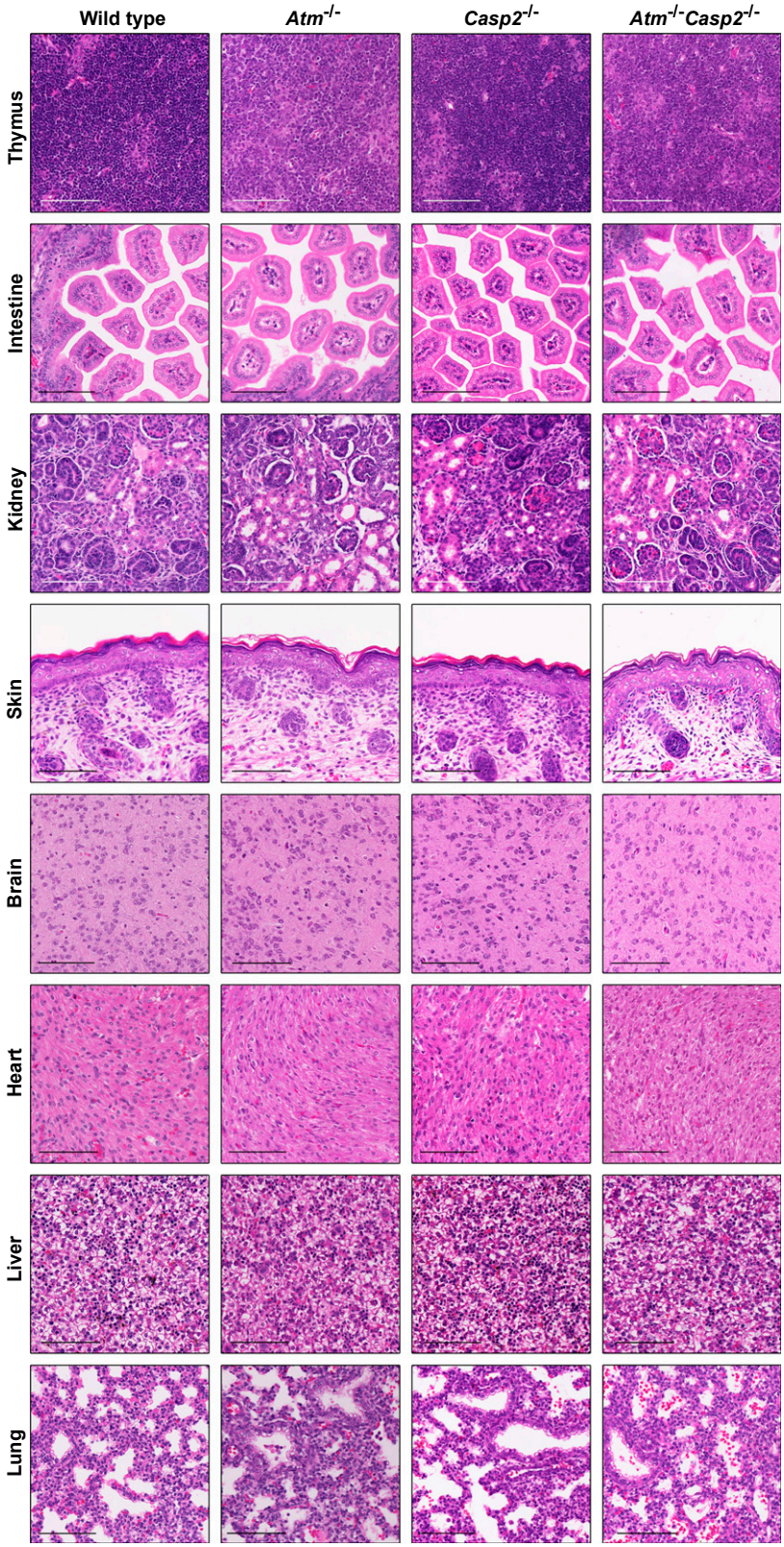

Fig. S2. Morphology of *Atm*$^{-/-}$*Casp2*$^{-/-}$ tissues. Representative images of H&E-stained, embryonic day 18.5 sagittal sections of brain, heart, liver, lung, thymus, intestine, kidney, and skin of the indicated genotypes. (Scale bar: 100 μm.)

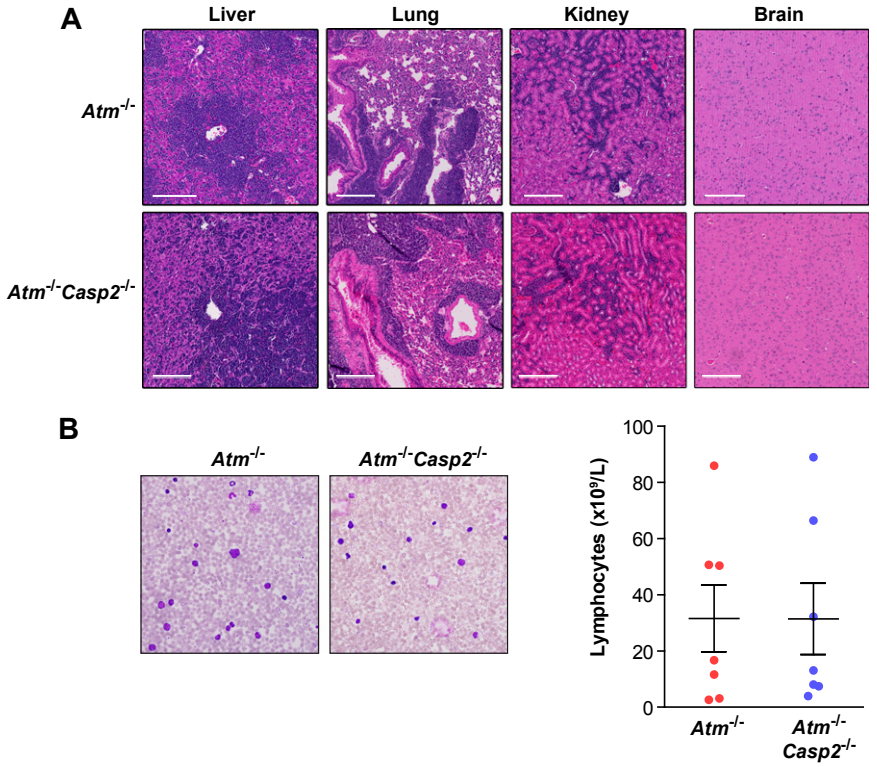

Fig. S3. Metastasis of $Atm^{-/-}$ and $Atm^{-/-}Casp2^{-/-}$ thymic lymphomas. (*A*) Representative images (magnification of 10×) of H&E-stained sections of lung, kidney, brain, and liver from tumor-laden mice showing metastatic infiltration. Liver, lung, and kidney showed extensive metastatic infiltration, whereas no metastasis was observed in the brain. (Scale bar: 200 μm.) (*B*) Peripheral blood lymphocyte counts and representative blood films (magnification of 40×) from tumor-laden $Atm^{-/-}$ ($n = 7$) and $Atm^{-/-}Casp2^{-/-}$ ($n = 7$) mice. Each point represents an individual mouse. Data presented as mean ± SEM.

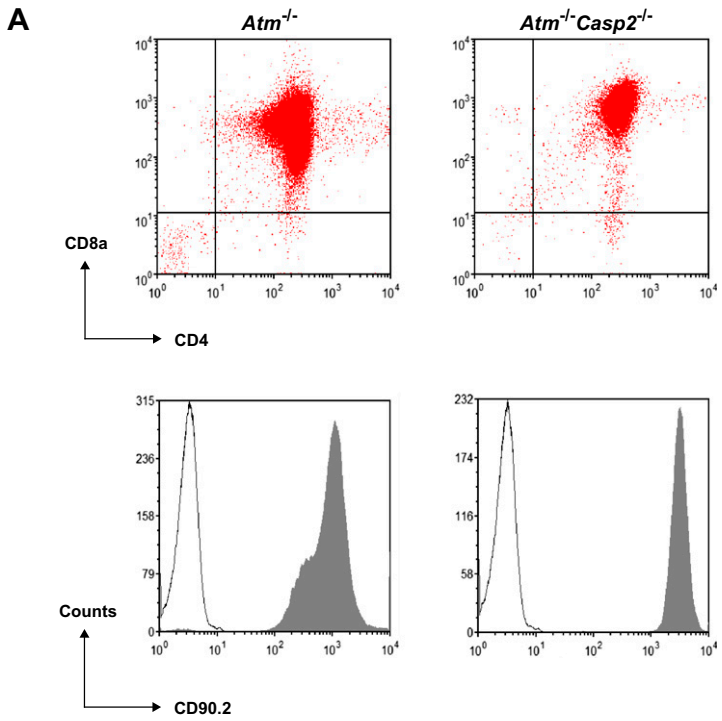

B

Genotype	%CD4$^-$CD8$^-$	%CD4$^-$CD8$^+$	%CD4$^+$CD8$^-$	%CD4$^+$CD8$^+$	%CD90.2$^+$
Atm$^{-/-}$ (n=3)	2.47 ± 0.68	1.69 ± 0.90	0.85 ± 0.40	95.00 ± 1.91	93.46 ± 3.28
Atm$^{-/-}$*Casp2*$^{-/-}$ (n=6)	1.00 ± 0.60	1.52 ± 0.59	1.11 ± 0.32	96.38 ± 0.80	96.72 ± 1.66

Fig. S4. Immunophenotyping of *Atm*$^{-/-}$ and *Atm*$^{-/-}$*Casp2*$^{-/-}$ thymic lymphomas. Flow cytometry analysis of CD4, CD8a, and CD90.2 (Thy1.2) expression in freshly isolated *Atm*$^{-/-}$ ($n = 3$) and *Atm*$^{-/-}$*Casp2*$^{-/-}$ ($n = 6$) thymic lymphomas. (*A*) Representative dot plots and 2D histograms (unshaded histogram represents negative control) and (*B*) quantification of expression of indicated markers. Data presented as mean ± SEM.

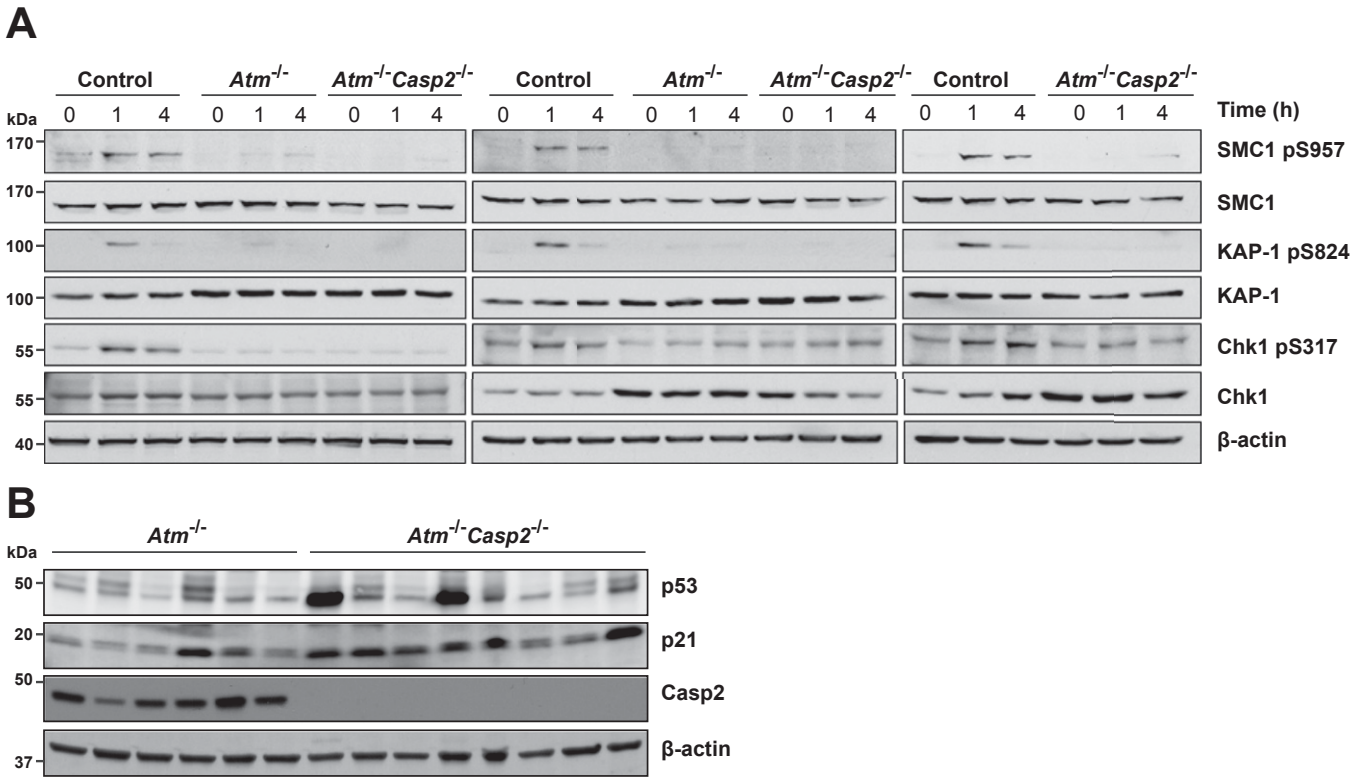

Fig. S5. DNA damage response in $Atm^{-/-}$ and $Atm^{-/-}Casp2^{-/-}$ thymic lymphomas. (*A*) Immunoblot analysis of SMC1, phospho-SMC1 (Ser-957), KAP-1, phospho-KAP-1 (Ser-824), Chk1, and phospho-Chk1 (Ser317) in $Atm^{-/-}$ (n = 2) and $Atm^{-/-}Casp2^{-/-}$ (n = 3) lymphoma cell lines following treatment with γ-radiation (5 Gy) at the indicated time points. Untreated and irradiated (5 Gy) EL4 cells (mouse thymoma cell line) cells were used as a positive control. (*B*) Immunoblot analysis of p53 and p21 in in $Atm^{-/-}$ (n = 6) and $Atm^{-/-}Casp2^{-/-}$ (n = 8) thymic lymphoma extracts. β-Actin is shown as loading control.

A Thymic Lymphomas

Genotype	Metaphases Analyzed	Metaphases with Indicated Chromosome Numbers																
		30	31	32	33	34	35	36	37	38	39	40	41	42	43	49	50-69	70-85
$Atm^{-/-}$ (n=3)	240	1				1			2	5	21	199	3	3				5
$Atm^{-/-}Casp2^{-/-}$ (n=8)	640				1	1	2	4	16	54	194	174	84	13	4	4	10	79

B Splenocytes

Genotype	Metaphases Analyzed	Metaphases with Indicated Chromosome Numbers																
		<30	31	32	33	34	35	36	37	38	39	40	41	42	43	44	50-69	70-90
Wild type (n=4)	200				1			1	1	1	9	174	9	3				1
$Casp2^{-/-}$ (n=4)	200	1			1	1		2	2	1	11	170	7	1	1			2
$Atm^{-/-}$ (n=3)	150				1	4		2	1	2	5	125	9					1
$Atm^{-/-}Casp2^{-/-}$ (n=5)	250	3			2	2	4	4	8	10	25	166	18			1	1	6

C Thymocytes

Genotype	Metaphases Analyzed	Metaphases with Indicated Chromosome Numbers																
		<30	31	32	33	34	35	36	37	38	39	40	41	42	43	44	50-69	70-90
Wild type (n=4)	200	1		1		1		1	1	8	18	157	6	1			2	3
$Casp2^{-/-}$ (n=4)	200		3		5	2	2	1	4	6	14	155	2	1			1	4
$Atm^{-/-}$ (n=3)	150	3		3		2	3	3	1	4	11	113	2				2	3
$Atm^{-/-}Casp2^{-/-}$ (n=5)	250	25	2	3	2	6	1	4	2	10	21	142	7	1		2	6	16

Fig. S6. Aneuploidy analysis in malignant and premalignant lymphocytes. Chromosome counts from metaphases derived from (*A*) thymic lymphomas, (*B*) premalignant splenocytes, and (*C*) premalignant thymocytes of the indicated genotypes.

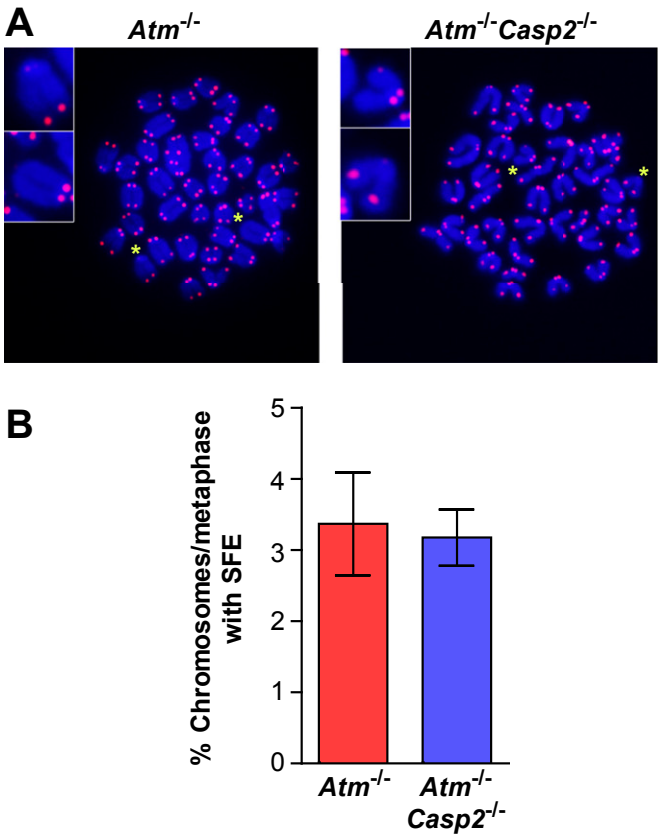

Fig. S7. Telomere analysis in $Atm^{-/-}$ and $Atm^{-/-}Casp2^{-/-}$ thymic lymphomas. (*A*) Representative fluorescent images (magnification of 100×) of metaphase spreads stained with a Cy3-conjugated PNA-telomere probe (red) and DAPI (blue). Yellow asterisks indicate chromosomes with signal-free ends (SFEs), with magnified images shown (*Inset*). (*B*) Quantification of chromosomes with SFEs in $Atm^{-/-}$ ($n = 3$) and $Atm^{-/-}Casp2^{-/-}$ ($n = 4$) thymic lymphomas. At least 50 metaphases were counted per tumor. Data presented as mean ± SEM.

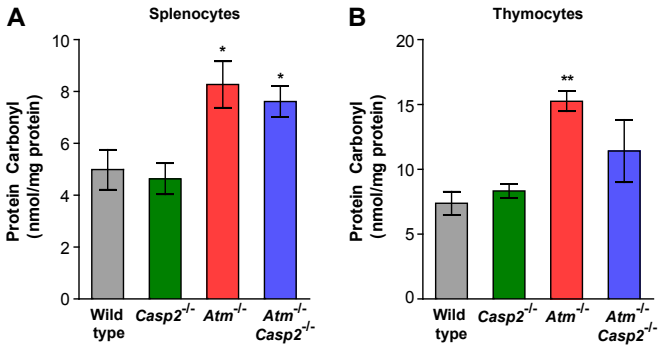

Fig. S8. Oxidative damage analysis in premalignant lymphocytes. Protein carbonyl measurements in (*A*) splenocytes and (*B*) thymocytes derived from premalignant WT ($n = 4$), $Casp2^{-/-}$ ($n = 4$), $Atm^{-/-}$ ($n = 3$), and $Atm^{-/-}Casp2^{-/-}$ ($n = 5$) mice. Data presented as mean ± SEM (*$P < 0.05$ and **$P < 0.01$ vs. WT controls, Student *t* test).

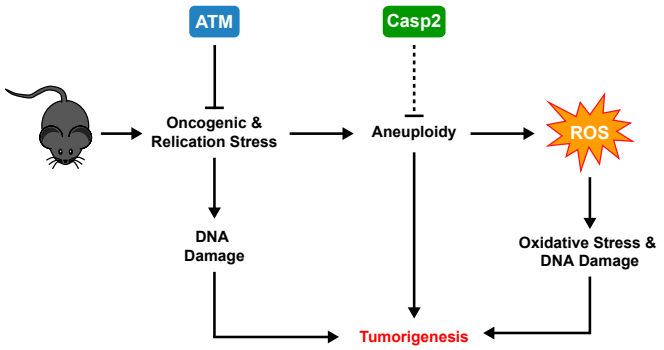

Fig. S9. A model for caspase-2 and ATM function in tumor suppression. ATM prevents DNA damage induced by oncogenic and replication stress through its well-established functions in DNA repair and cell cycle arrest. Therefore, in the absence of ATM, cells accumulate DNA damage, which promotes mutagenesis and tumorigenesis. Caspase-2 is important for suppressing aneuploidy and the associated oxidative stress, thereby providing a protective barrier against tumorigenesis in *Atm*-deficient cells. Therefore, combined deletion of *Atm* and *caspase-2* promotes aneuploidy and exacerbates oxidative stress, thereby accelerating tumorigenesis.